

## Novel Pressure-Induced Magnetic Transition in Magnetite ( $\text{Fe}_3\text{O}_4$ )

Yang Ding,<sup>1,\*</sup> Daniel Haskel,<sup>2</sup> Sergei G. Ovchinnikov,<sup>3,4</sup> Yuan-Chieh Tseng,<sup>2</sup>  
Yuri S. Orlov,<sup>4</sup> Jonathan C. Lang,<sup>2</sup> and Ho-kwang Mao<sup>1,5,6</sup>

<sup>1</sup>*HPSynC, Carnegie Institution of Washington, 9700 South Cass Avenue, Argonne, Illinois 60439, USA*

<sup>2</sup>*Advanced Photon Source, Argonne National Laboratory, Argonne, Illinois 60439, USA*

<sup>3</sup>*Kirensky Institute of Physics, Siberian Branch of Russian Academy of Science, 660036 Krasnoyarsk, Russia*

<sup>4</sup>*Siberian Federal University, Krasnoyarsk, 660041 Russia*

<sup>5</sup>*Geophysical Laboratory, Carnegie Institution of Washington, 5251 Broad Branch Road NW, Washington, DC 20015, USA*

<sup>6</sup>*HPCAT, Carnegie Institution of Washington, Building 434E, 9700 South Cass Avenue, Argonne, Illinois 60439, USA*

(Received 9 May 2007; revised manuscript received 13 November 2007; published 1 February 2008)

Fe  $K$ -edge x-ray magnetic circular dichroism of magnetite ( $\text{Fe}_3\text{O}_4$ ) powders was measured with synchrotron radiation under variable pressure and temperature conditions in diamond anvil cell. The magnetic dichroism was observed to decrease discontinuously by  $\sim 50\%$  between 12 and 16 GPa, independent of temperature. The magnetic transition is attributed to a high-spin to intermediate-spin transition of  $\text{Fe}^{2+}$  ions in the octahedral sites and could account for previously observed structural and electrical anomalies in magnetite at this pressure range. The interpretation of x-ray magnetic circular dichroism data is supported by x-ray emission spectroscopy and theoretical cluster calculations.

DOI: [10.1103/PhysRevLett.100.045508](https://doi.org/10.1103/PhysRevLett.100.045508)

PACS numbers: 62.50.-p, 75.50.Bb, 78.70.Dm

Magnetite ( $\text{Fe}_3\text{O}_4$ ), the oldest known magnet, has an inverse spinel structure with the formula of  $\text{Fe}^{3+}_{(\text{Td})}(\text{Fe}^{2+}\text{Fe}^{3+})_{(\text{Oh})}\text{O}_4$ . The magnetic moments on tetrahedral (Td) and octahedral (Oh) sites couple antiferromagnetically resulting in a ferrimagnet with a net saturation magnetic moment of  $4\mu_B$  per formula unit, as confirmed by experimental measurement of  $4.07\mu_B$  [1]. Recently, a set of high-pressure electrical, Mössbauer, and x-ray diffraction measurements conducted on magnetite, partly directed at decoding the origin of the Verwey transition (VT) [2,3], disclosed a complex behavior of pressure- and temperature-dependent behaviors. In addition to reports that the temperature-induced VT vanishes at high pressure [4,5] and an electrical resistivity anomaly between 12–16 GPa at room temperature [6], an inverse ( $I$ ) to normal ( $N$ ) spinel ( $\text{Fe}^{2+}_{(\text{Td})}2\text{Fe}^{3+}_{(\text{Oh})}\text{O}_4$ ) transition was proposed in Refs. [7,8] to explain Mössbauer spectroscopy and x-ray diffraction measurements under various  $P$ - $T$  conditions. The proposed  $I$ - $N$  transition should result in a 50% increase in net magnetic moment, but this increase was not observed by neutron powder diffraction [9] or single-crystal x-ray diffraction [10] measurements.

We carried out synchrotron-based x-ray magnetic circular dichroism (XMCD) measurements at variable  $P$ - $T$  conditions to examine the magnetic properties of magnetite in the pressure range where the reported electronic and magnetic transitions occur. Compared with other probes of magnetism at high pressure, including Mössbauer spectroscopy, ac susceptibility, and x-ray emission spectroscopy, XMCD is a particularly powerful local probe that does not require isotope enrichment and can readily be applied to the study of ferro(i)magnetic materials [11]. Our XMCD measurements revealed a pressure-induced magnetic transition at 12–16 GPa which is independent of

temperature within the 40–300 K range. We suggest that this magnetic transition is associated with a high-spin (HS) to intermediate-spin (IS) transition of  $\text{Fe}^{2+}$  ions in the Oh sites of magnetite, and the suggestion is further supported by our independent x-ray emission spectroscopy (XES) measurements and theoretical cluster calculations. Our results are inconsistent with the proposed  $I$ - $N$  spinel transition of Refs. [7,8].

The XMCD measurements were performed at undulator beam line 4ID-D of the Advanced Photon Source (APS), Argonne National Laboratory. Details on beam line optics and instrumentation can be found in Refs. [12,13]. Magnetite samples were micrometer-sized powders ground from high-quality single crystals with 99.999% purity. The powders, mixed with pressure standard Cu powders and pressure transmitting medium silicon oil, were loaded into a symmetrical membrane driven CuBe cell with perforated diamond anvils. Pressures were calibrated based on the pressure shift of x-ray absorption fine structure (XAFS) of the Cu  $K$  edge [13].

In the experiments, the energy of the incident x-ray beam was scanned through the Fe  $K$ -absorption edge (7112 eV) to acquire both the x-ray absorption near edge structure (XANES) and XMCD spectra in helicity-switching mode. The data were collected from 4.2 GPa to 18.1 GPa (with  $\sim 4$  GPa intervals) with temperature varying from 20 K to 300 K (with  $\sim 60$  K intervals) at each pressure point [13].

The XES and powder diffraction experiments were performed on magnetite powders with helium as pressure medium in a Mao-type diamond anvil cells, at the 16ID-D and -B stations of HPCAT sector, APS, respectively. For XES, the incident monochromatic x-ray beam was set at 7.18 keV and the Fe  $K_\beta$  emission spectra were scanned

using a Si(333) crystal analyzer and Si(Sn) x-ray detector collecting in a backscattering geometry [14]. For powder diffraction experiments, NaCl powders were mixed with magnetite in a diamond anvil cell to monitor the condition of hydrostaticity.

Figure 1 shows the normalized Fe *K*-edge XANES and XMCD spectra collected from magnetite samples at 40 K from 4.2 GPa to 18.2 GPa. Two distinct pairs of negative and positive peaks appear in the XMCD spectra; they are labeled in Fig. 1(b) as *A-A'* ( $E = 7.112\text{--}7.113$  keV) and *B-B'* ( $E = 7.123\text{--}7.129$  keV), respectively. These two magnetic components are the result of the difference XANES spectra for opposite x-ray helicity at positions *A-A'* and *B-B'* in Fig. 1(a), respectively. Figure 2 is a plot of the intensity of peaks *A-A'* and *B-B'* under various pressure and temperature conditions. Below 12.2 GPa, no appreciable change can be detected in either XANES or XMCD spectra, even when the temperature drops below the Verwey transition temperature (which is pressure dependent) [4,5] at each pressure point, indicating that the Verwey transition does not involve changes in magnetic moment. However, above 12.2 GPa, the intensities of *A-A'* and *B-B'* drop by  $\sim 50\%$  at 16.2 GPa while no change occurs in the corresponding XANES spectra, signifying a magnetic transition between 12–16 GPa [Fig. 1(a)]. The pressure-induced magnetic transition is independent of

temperature within the range from 40 to 300 K (Fig. 2). X-ray diffraction in the same pressure range shows no structural phase transition except peak broadening starting above 10 GPa even with the magnetite sample in hydrostatic (helium) pressure medium.

The *K*-edge XMCD depends on the spin and orbital polarization of the projected, unoccupied *4p* final states. It is generally accepted that the spin polarization of *4p* states arises predominately from on-site and intrasite exchange interactions with polarized *3d* states [15–21]. Accordingly, changes in *3d* polarization directly affect the *K*-edge XMCD. Although a complete interpretation of the energy dependence of Fe *K*-edge XMCD spectra in terms of contributions from distinctive Td and Oh crystallographic sites is still lacking, there is mounting evidence that peaks *A-A'* are predominately associated with Td sites while both sites contribute significantly to peaks *B-B'* [22]. We observed roughly equal, half reductions of *A-A'* and *B-B'* peaks during the transition in our repeated experiments, which indicates a correlated reduction in Fe *4p* magnetic polarization at both Td and Oh sites. While the XMCD magneto-optical sum rule for the *K* edge only relates to the expectation value of the orbital moment per *4p* hole [23], it is reasonable to argue that our data indicate a reduction in half of the net magnetic moment of magnetite between 12.2 and 16.2 GPa. As discussed below, we explored a number of possible mechanisms to explain the observed magnetic transition and conclude that the most likely is a HS to IS transition at the  $\text{Fe}^{2+}$  (Oh) sites. In fact, experiments [24] and calculations [25–28] indicate that the average net moment of magnetite arises predominately from the minority spin band associated with  $\text{Fe}^{2+}$  (Oh) sites.

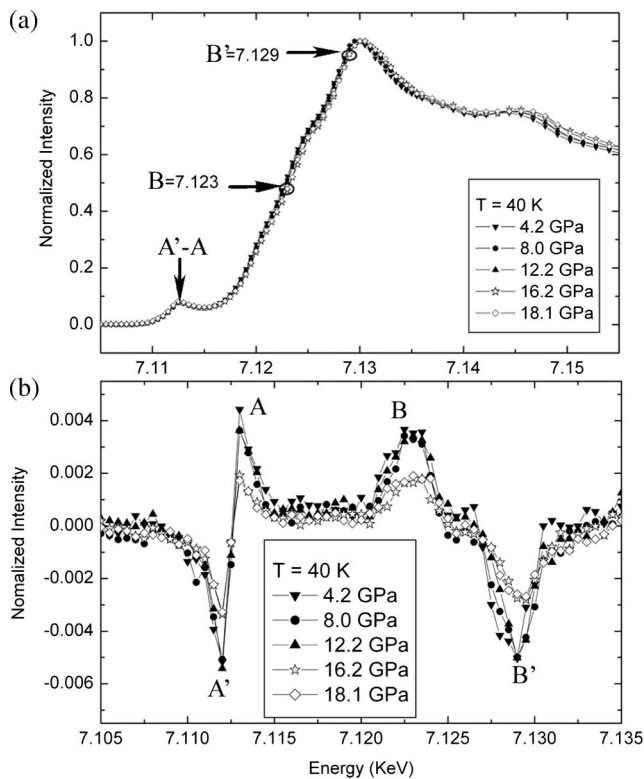


FIG. 1. (a) The normalized XANES of magnetite collected at 40 K from 4.2 GPa to 18.1 GPa. (b) The corresponding normalized XMCD at the same *P-T*.

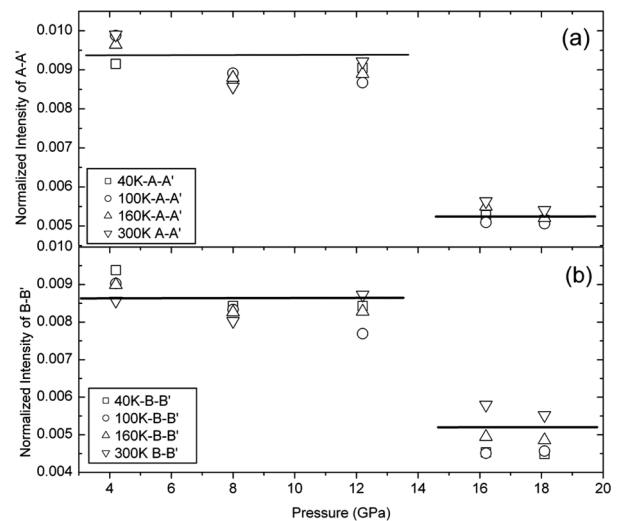


FIG. 2. The plot of intensity of XMCD peaks (a) *A-A'* and (b) *B-B'* from 4.2 GPa to 18.1 GPa at 40, 100, 160, and 300 K. The intensity drops drastically between 12 and 16 GPa. The lines are drawn to guide the eyes for intensity levels before and after the transition.

We calculated multielectron energy levels of HS, IS, and low spin (LS) states of  $\text{Fe}^{2+}$  ion using exact diagonalization of the multiband  $p$ - $d$  model Hamiltonian for the  $\text{FeO}_6$  cluster, similar to the study of  $\text{CoO}_6$  cluster for  $\text{LaCoO}_3$  [29]. The  $\text{Co}^{3+}$  in  $\text{CoO}_6$  octahedra and  $\text{Fe}^{2+}$  in  $\text{FeO}_6$  octahedra have the same electronic configuration but different parameters of the Hamiltonian. By rescaling parameters, such as hopping  $tpd$ ,  $tpp$ , Coulomb  $Vpd$ , and crystal field  $Dq$ , from the  $\text{CoO}_6$  set, we obtained their pressure dependence for  $\text{FeO}_6$ . The calculated energy level scheme is shown in Fig. 3(d), where the HS is the ground state at  $P = 0$  ( $10Dq = 2.40$  eV) and the Hund exchange coupling (0.65 eV) was fitted to get the HS-IS crossover of  $\text{Fe}^{2+}$  at 15 GPa ( $10Dq = 2.53$  eV), which confirms our interpretation of the experimental results. Calculations for  $\text{Fe}^{3+}$  in Td and Oh sites with the same parameters revealed the HS of  $\text{Fe}^{3+}$  state remains stable until 50 GPa. The origin of HS-IS crossover in  $\text{Fe}^{2+}$  is attributed to the covalence effect, or in another word,  $3d(\text{Fe})$ - $2p(\text{O})$  hybridization induced by pressure. Because of this effect, the stabilization of the HS, IS, and LS under high pressure is affected by the competition among crystal field splitting, Hund exchange coupling, and  $3d$ - $2p$  hopping energy. At certain pressure, IS can become more stable than LS or HS,

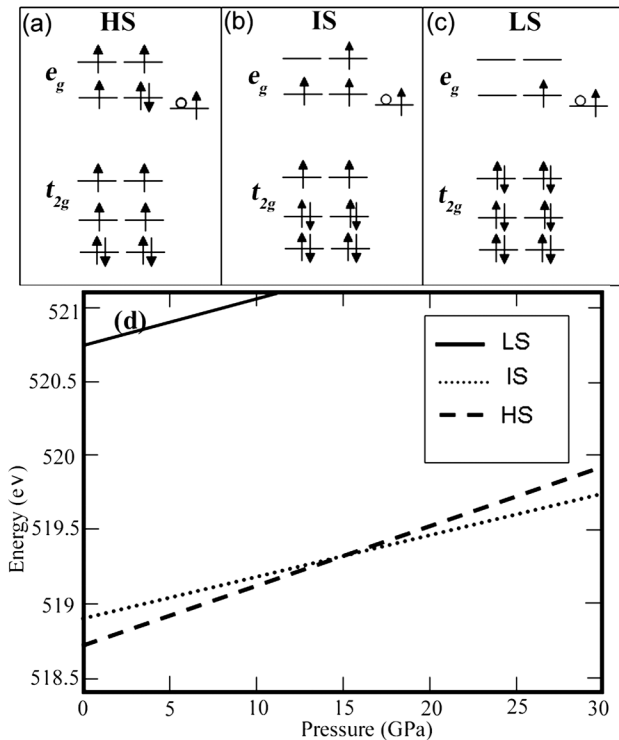


FIG. 3. Schematic representation of  $\text{Fe}^{2+} d^6 + d^7L$  configuration in (a) high-spin state ( $S = 2$ ), (b) intermediate-spin state ( $S = 1$ ), and (c) low-spin state ( $S = 0$ ). In (a), (b), and (c), the left side of column is the  $d^6$  configuration, while the right side represents the  $d^7L$ . The  $\circ$  denotes a hole in the oxygen  $p$  shell. (d) High-pressure dependent energy levels of high-, intermediate-, and low-spin states at 300 K.

when the energy gain from  $d$ - $p$  hybridization becomes a leading term. A similar example has been demonstrated by Korotin *et al.* in  $\text{LaCoO}_3$  [30]. Another way to stabilize the IS could arise from negative charge-transfer energy as shown for  $\text{Co}^{+4}$  ion in  $\text{SrCoO}_3$  [31].

Other possible mechanisms that were considered include orbital transitions, HS-LS, and charge disproportionation (e.g., inverse-normal spinel transition) for  $\text{Fe}^{3+}$  or  $\text{Fe}^{2+}$  at Td or Oh site, but these could not successfully explain the large, discontinuous reduction of the net average magnetic moment. The spin transition reduces the population of  $e_g$  electrons, which are major conducting electrons in magnetite, and could be the cause for the electrical anomaly observed between 12–16 GPa pressure range [6]. Though the authors attributed the anomaly to a structural transition, no evidence for such transition is seen by x-ray diffraction in this pressure range [32,33].

To further confirm the spin transition suggested from XMCD results, we conducted an independently XES experiment at room temperature. As shown in Fig. 4, the emission spectrum of HS Fe is characterized by a main peak  $K_{\beta 1,3}$  with the energy of 7058 eV and a satellite peak  $K_{\beta}'$  located at lower energy appearing as a result of the  $3p$  core-hole- $3d$  exchange. The intensity of  $K_{\beta}'$  is proportional to the number of unpaired  $3d$  electrons which decreases at a spin transition, and is often used as a diagnostic probe for pressure-induced HS-IS-LS transition [14,34–38]. In the present study, a dip at 15.8 GPa was observed in XES, evidencing a transient state possibly associated with a HS-IS spin transition. Once pressure was raised above the observed XMCD transition point to 16.5 and 20.6 GPa, the overall  $K_{\beta}'$  intensity drops  $\sim 15\%$  relative to that below the transition at 13.5 GPa (Fig. 4). The drop of  $K_{\beta}'$  is consistent with HS-IS picture. Only two out of the total 14

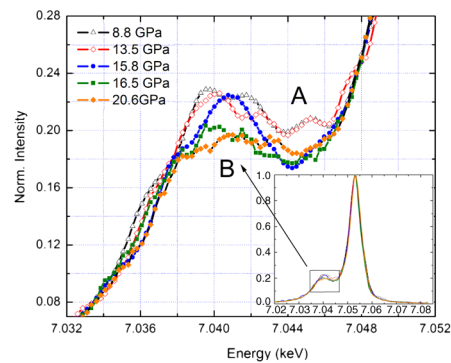


FIG. 4 (color online). The  $K_{\beta}'$  satellites from high-pressure XES measurement on magnetite from 8.8 to 20.6 GPa. The instrument resolution (FWHM) is 1 eV. The inset is a complete  $K_{\beta}$  XES spectra, while the  $K_{\beta}'$  satellite is enlarged in the figure. The integrated  $K_{\beta}'$  intensity above 15.8 GPa (16.5 and 20.6 GPa) is 15% lower than that below 15.8 GPa (8.8 and 13.5 GPa). The changes in XES are consistent with the interpretation of HS-IS transition in  $\text{Fe}^{2+}$  while the two  $\text{Fe}^{3+}$  remain HS.

unpaired electrons in the HS state of  $\text{Fe}_3\text{O}_4$ , i.e., four in  $\text{Fe}^{2+}$  and ten in  $\text{Fe}^{3+}$ , pair at HS-IS transition, corresponding to  $\sim 15\%$  reduction of total unpaired electrons.

Our XMCD experiments showing a 50% reduction in net magnetic moment, together with other recent diffraction studies [9,10], are inconsistent with the  $I$ - $N$  transition proposed in Refs. [7,8].

The XMCD experiments were conducted at beam line 4ID-D of XOR and the x-ray emission experiments were performed at 16ID-D beam line of HPCAT, APS, Argonne National Laboratory. We thank Guoyin Shen, Paul Chow, Yuming Xiao, and Lin Wang's help on the beam line assistance at HPCAT, and Michel Van Veenendaal and Eiji Kaneshita's help on the discussion. Use of the HPCAT facility was supported by DOE-BES, DOE-NNSA (CDAC), NSF, and the W.M. Keck Foundation. Use of the APS was supported by DOE-BES, under Contract No. DE-AC-02-06CH11357. Theoretical calculations were supported by RFBR Grant No. 07-02-00226 and by the Presidium of Russian Academy of Science Program "Quantum Macrophysics".

---

\*yangding@aps.anl.gov

- [1] P. Weiss and R. Forrer, *Ann. Phys. (Paris)* **12**, 279 (1929).
- [2] J. García and G. Subías, *J. Phys. Condens. Matter* **16**, R145 (2004).
- [3] E. J. W. Verwey, *Nature (London)* **144**, 327 (1939).
- [4] G. Kh. Rozenberg, G. R. Hearne, and M. P. Pasternak, *Phys. Rev. B* **53**, 6482 (1996).
- [5] S. Todo, N. Takeshita, T. Kanehara, T. Mori, and N. Mori, *J. Appl. Phys.* **89**, 7347 (2001).
- [6] E. R. Morris and Q. Williams, *J. Geophys. Res.* **102**, 18139 (1997).
- [7] M. P. Pasternak, W. M. Xu, G. Kh. Rozenberg, R. D. Taylor, and R. Jeanloz, *J. Magn. Magn. Mater.* **265**, L107 (2003).
- [8] G. Kh. Rozenberg, Y. Amiel, W. M. Xu, M. P. Pasternak, R. Jeanloz, M. Hanfland, and R. D. Taylor, *Phys. Rev. B* **75**, 020102 (2007).
- [9] S. Klotz, T. Straessle, G. Rousse, G. Hamel, and T. Hansen, in *Joint 21st AIRAPT and 45th EHPRG International Conference on High Pressure Science and Technology, Catania, Italy, 2007*, p. 182.
- [10] G. D. Gatta, I. Kantor, T. B. Ballaran, L. Dubrovinsky, and C. McCammon, *Phys. Chem. Miner.* **34**, 627 (2007).
- [11] E. Duman, M. Acet, E. F. Wassermann, J. P. Itié, F. Baudelet, O. Mathon, and S. Pascarelli, *Phys. Rev. Lett.* **94**, 075502 (2005); O. Mathon, F. Baudelet, J.-P. Me, S. Pasternak, A. Polian, and S. J. Pascarelli, *J. Synchrotron Radiat.* **11**, 423 (2004).
- [12] J. W. Freeland, J. C. Lang, G. Srajer, R. Winarski, D. Shu, and D. M. Mills, *Rev. Sci. Instrum.* **73**, 1408 (2002).
- [13] D. Haskel, Y. C. Tseng, J. C. Lang, and S. Sinogeikin, *Rev. Sci. Instrum.* **78**, 083904 (2007).
- [14] J.-F. Lin, V. V. Struzhkin, S. D. Jacobsen, M. Y. Hu, P. Chow, J. Kung, H. Liu, H. K. Mao, and R. J. Hemley, *Nature (London)* **436**, 377 (2005).
- [15] G. Schütz, W. Wagner, W. Wilhelm, P. Kienle, R. Zeller, R. Frahm, and G. Materlik, *Phys. Rev. Lett.* **58**, 737 (1987).
- [16] H. Sakurai, F. Itoh, H. Maruyama, A. Koizumi, K. Kobayashi, H. Yamazaki, Y. Tanji, and H. Kawata, *J. Phys. Soc. Jpn.* **62**, 459 (1993).
- [17] S. Stähler, G. Schütz, and H. Ebert, *Phys. Rev. B* **47**, 818 (1993).
- [18] I. Harada and A. Kotan, *J. Phys. Soc. Jpn.* **63**, 1285 (1994).
- [19] J. Igarashi and K. Hirai, *Phys. Rev. B* **50**, 17820 (1994).
- [20] C. Brouder, M. Alouani, and K. H. Bennemann, *Phys. Rev. B* **54**, 7334 (1996).
- [21] G. Y. Guo, *Phys. Rev. B* **55**, 11619 (1997).
- [22] A. Cady, D. Haskel, J. C. Lang, Z. Islam, G. Srajer, A. Ankudinov, G. Subías, and J. García, *Phys. Rev. B* **73**, 144416 (2006); site-specific FEFF8.0 calculations support this conclusion.
- [23] H. Ebert, in *Spin-Orbit Influenced Spectroscopies*, edited by H. Ebert and G. Schütz (Springer, New York, 1996), p. 160.
- [24] E. Goering, S. Gold, M. Lafkioti, and G. Schütz, *Europhys. Lett.* **73**, 97 (2006).
- [25] A. Yanase and K. Siratori, *J. Phys. Soc. Jpn.* **53**, 312 (1984).
- [26] Z. Zhang and S. Satpathy, *Phys. Rev. B* **44**, 13319 (1991).
- [27] M. Pénicaud, B. Siberchicot, C. B. Sommers, and J. Kubler, *J. Magn. Magn. Mater.* **103**, 212 (1992).
- [28] V. N. Antonov, B. N. Harmon, and A. N. Yaresko, *Phys. Rev. B* **67**, 024417 (2003).
- [29] S. G. Ovchinnikov and Yu S. Orlov, *JETP* **104**, 436 (2007).
- [30] M. A. Korotin, S. Yu. Ezkov, I. V. Solovyev, V. I. Anisimov, D. I. Khomskii, and G. A. Sawatzky, *Phys. Rev. B* **54**, 5309 (1996).
- [31] M. Potze, G. Sawatzky, and M. Abbate, *Phys. Rev. B* **51**, 11501 (1995).
- [32] H. K. Mao, T. Takahashi, W. Bassett, G. L. Kinsland, and L. Merrill, *J. Geophys. Res.* **79**, 1165 (1974).
- [33] Y. Fei, D. J. Frost, H. K. Mao, C. T. Prewitt, and D. Häusermann, *Am. Mineral.* **84**, 203 (1999).
- [34] L. S. Dubrovinsky, N. A. Dubrovinskaia, C. McCammon, G. Kh. Rozenberg, R. Ahuja, J. M. Osorio-Guillen, V. Dmitriev, H.-P. Weber, T. Le Bihan, and B. Johansson, *J. Phys. Condens. Matter* **15**, 7697 (2003).
- [35] J.-P. Rueff, C.-C. Kao, V. V. Struzhkin, J. Badro, J.-F. Shu, R. J. Hemley, and H. K. Mao, *Phys. Rev. Lett.* **82**, 3284 (1999).
- [36] J. Badro, G. Fiquet, F. Guyot, J.-P. Rueff, V. V. Struzhkin, G. Vankó, and G. Monaco, *Science* **300**, 789 (2003).
- [37] J. Badro, J.-P. Rueff, G. Vanko, G. Monaco, G. Fiquet, and F. Guyot, *Science* **305**, 383 (2004).
- [38] J. Li, V. V. Struzhkin, H. K. Mao, J. Shu, R. J. Hemley, Y. Fei, B. Mysen, P. Dera, V. Prakapenka, and G. Shen, *Proc. Nat. Acad. Sci.* **101**, 14027 (2004).